

Effect of annealing treatment and deposition temperature on CdS thin films for CIGS solar cells applications

Ravi Kant Choubey¹ · Dipti Desai² · S. N. Kale² · Sunil Kumar³

Received: 11 September 2015 / Accepted: 4 April 2016 / Published online: 12 April 2016
© Springer Science+Business Media New York 2016

Abstract Present study expounds how post-deposition annealing affects the various structural and optical properties of CdS thin films deposited by chemical bath deposition technique. The structural and morphological changes have been observed by X-ray diffraction (XRD), field emission scanning electron microscopy, Transmission electron microscopy and atomic force microscopy studies; however, the optical and electrical properties of the as deposited and annealed films were studied by UV–Vis spectroscopy and four probe method, respectively. The energy dispersive X-ray analysis confirmed that all as-deposited and annealed films showed almost stoichiometric composition. XRD pattern of the thin films clearly shows the transformation from the cubic structure to the hexagonal structure induced by annealing. The band gaps of the as deposited films were found in the range of 2.41–2.47 eV, while after annealing it decreases due to the decomposition of hydroxides. The electrical resistivity found to decrease approximately 10 times after annealing the as-deposited CdS thin films.

1 Introduction

It is well known that crystalline silicon solar cells have good efficiency, but their uses are restricted due to the high cost. Hence, the efforts were done to develop new technology which is cost efficient; this led to the idea of Thin-film solar cells. Thin-film solar technology offer several advantages over traditional silicon panels such as less bulky and easy incorporation into existing structures. Amongst all the thin film solar cells CIGS (Cu(In,Ga)Se_2) is one of the most promising materials because such photovoltaic module having several key features for example high efficiency, stability, low cost and adaptability to various applications [1]. Recently, the record efficiency for CIGS cells is close to 21.7 %, which has been achieved by Centre for Solar Energy and Hydrogen Research group, ZSW [2]. During the manufacturing of these solar cells, the p-n heterojunction is formed by depositing a thin n-type buffer layer of CdS which plays an important role.

CdS films have been prepared by various techniques such as sputtering [3], MOCVD [4], close space sublimation (CSS) [5, 6], chemical bath deposition (CBD) [7–9], spray pyrolysis [10], pulsed-laser deposition [11] etc. Among all those methods, CBD is most widely used deposition technique for CdS thin films. The main interest in depositing CdS via CBD, stems from the fact this growth method yields stable, adherent and hard CdS films with good reproducibility [12]. Beside, there is no sophisticated instrumentation needed and the synthesis of the films is very simple.

In spite of the deposition technique, the quality of the deposited films and optimization of the deposition process is still an open subject. Several studies have been carried out to produce CdS thin films with good optoelectronic properties appropriate for photovoltaic devices. For the above mentioned purpose, few necessary properties for the

✉ Ravi Kant Choubey
ravikantchoubey@gmail.com

¹ Department of Applied Physics, Amity Institute of Applied Sciences (AIAS), Amity University, Noida Campus, Sector-125, Noida, U.P. 201 313, India

² Department of Applied Physics, Defence Institute of Advanced Technology, Girinagar, Pune 411025, India

³ Quantum Functional Semiconductor Research Center, Dongguk University, Seoul 100715, South Korea

CdS thin films are: (1) high transparency (2) not too thin to avoid the short circuiting and high conductivity.

Many research groups have studied and demonstrated several CBD procedures to produce CdS thin films. In fact most CBD depositions have been carried out at temperatures and pH between 70–90 and 10–12 °C, respectively [8, 13, 14]. However, CdS films deposited by CBD tend to form the cubic phase, having poor crystalline quality. Hence, the crystalline quality and other properties can be improved by the annealing treatment. In last some years, many groups have reported the improved properties of the CdS thin films by annealing in different atmospheres [15, 16]. Recently, Han et al. [17] have reported the annealing effects on the chemical deposited CdS films and found that the performance of the solar cell increases when CdS is annealed with oxygen as compare to the CdS is annealed with argon–hydrogen. Recently, exciton dynamics of CdS films have been investigated using ultrafast laser spectroscopy by Cooper et al. [18] while structural, optical and magnetic properties of Ni-doped CdS thin films have been studied by Premarani et al. [19]. Also, a composite window layer of the sandwich structure containing CdS/ZnS multilayer for CdTe thin film solar cell has been designed by Liu et al. [20].

The present work describes the deposition of CdS thin films via CBD at four different deposition temperatures (70, 75, 80 and 85 °C) and elucidates the improvement in CdS thin films by annealing in air atmosphere. The evolution of the optical, structural, morphological and electrical properties of the annealed films have been studied by energy dispersive X-ray analysis (EDS), X-ray diffraction (XRD), UV–visible spectroscopy, field emission scanning electron microscopy (FE-SEM), transmission electron microscopy (TEM), atomic force microscopy (AFM) and four probe method.

2 Experimental

2.1 Chemical bath deposition

All the chemicals have been purchased from Sigma Aldrich having purity $\geq 99.0\%$. CdS films were deposited on soda lime glass substrates of size 76 mm \times 16 mm \times 1 mm. The cleaning of the glass slides is most important part, before it is used as a substrate for the film deposition. Glass substrates were cleaned in an ultrasonic water bath for 20 min and then dipped in HCL and acetone for 5–10 min independently. Finally, slides were rinsed with DI water and dried in oven before use as substrate.

A substrate Holder was made such that four substrates can be introduced at a time with their back sides facing each other into the chemical bath solutions. The deposition arrangement consisted of a water bath on a hot plate. We

used a 300 ml borosilicate glass flat bottom beaker (100 mm diameter) for CdS deposition. The CdS thin films were deposited onto glass slides from an aqueous chemical bath containing 0.06 M cadmium sulfate ($\text{CdSO}_4 \cdot 5\text{H}_2\text{O}$), 0.12 M thiourea ($\text{CS}(\text{NH}_2)_2$), and 1.74 M ammonia (NH_3). Here, CdSO_4 and $\text{CS}(\text{NH}_2)_2$ were used as a sources of Cd and S, respectively while ammonia was used as complexing agent. The pH of the solution was adjusted and fixed to 11 by adding the ammonia solution drop wise to the CdSO_4 solution, and then thiourea was added to it. Immediately after the addition of thiourea, the pre-cleaned glass substrates were vertically immersed into the chemical bath solution. The reactions were carried out at temperatures 70, 75, 80 and 85 °C, for 80 min. The mixture was stirred continuously at 200 rpm during the deposition process. At the end of the deposition process, the substrates were removed from the chemical bath. The deposited CdS films were washed ultrasonically to remove the loosely adhered CdS particles on the film and finally dried in air. To observe the effect of annealing, the films were heat treated at 400 °C for 20 min in air, in furnace.

2.2 Characterizations

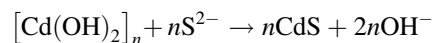
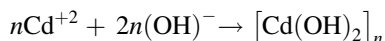
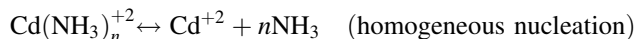
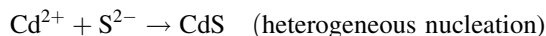
The structural characterization of the films was carried out by the X-ray diffraction (XRD) technique using D8 advance (Bruker). The operating conditions were as follows: target $\text{Cu-}k_{\alpha 1}$, voltage 40 kV, current 40 mA, scan range 10°–60°, step size: 0.02°. The films grain size was estimated from the XRD pattern analysis. The transmission spectra were recorded in the range of 350–1100 nm by a UV–visible–NIR spectrophotometer (SPECORD[®] 210 plus, Germany). The surface morphology of the CdS films were analyzed by FE-SEM (Model: Sigma, Carl Zeiss), HRTEM (Model: JEOL 2010) and AFM (Model: MFP 3D, Asylum Research). Thickness of the films was measured by surface profiler (Model: XP-1, Ambios Technology) having 1A° resolution. The four point probe method (Keithley 2400 source meter) was used to measure the resistivity of the as deposited as well as annealed CdS thin films. In order to perform the resistivity measurements, the samples were first cut into 1 cm \times 1 cm squares and silver contacts were given at each corner of the film. All contacts were tested prior to measurement.

3 Results and discussion

3.1 Film growth and composition analysis

The formation of the CdS takes place mainly through two processes: (1) heterogeneous nucleation (on the glass surface) and (2) homogeneous nucleation (in the solution due

to the spontaneous precipitation of CdS). The homogeneous deposition is highly undesirable since it results the formation of powdery and non-adherent films. The rate of CdS formation can be controlled by bath temperature and pH of the solution. For good quality films, heterogenous process is highly desirable, in which adsorption of Cd^{2+} and S^{2-} ions takes place. The reactions for both the processes are given as follows:



All the as-deposited films were mostly yellow in color, smooth and adherent; scanning electron micrographs showed uniform microstructure of the film surface. It was observed that the thickness slightly increases after annealing. Thickness of as deposited films was found to be in the range of 70 nm while after annealing it was found 80 nm.

The EDS technique was used to estimate the composition of the as deposited and annealed CdS thin films. Figure 1 shows the average atomic ratio of Cd/S as a function of deposition temperature. It can be observed that Cd/S ratio varies in the range of 1.11–1.13 in as deposited CdS thin films while after annealing the Cd/S ratio increases and varied from 1.18 to 1.21. Cortes et al. [21] have also observed Cd/S ratio approximately 1.2 in CdS thin films annealed at 450 °C. The increase in Cd/S ratio indicates that sulfur vacancies are created which can be due to the coexistence of CdS with other cadmium compounds, which are also intermediates or products of the CBD reaction [22].

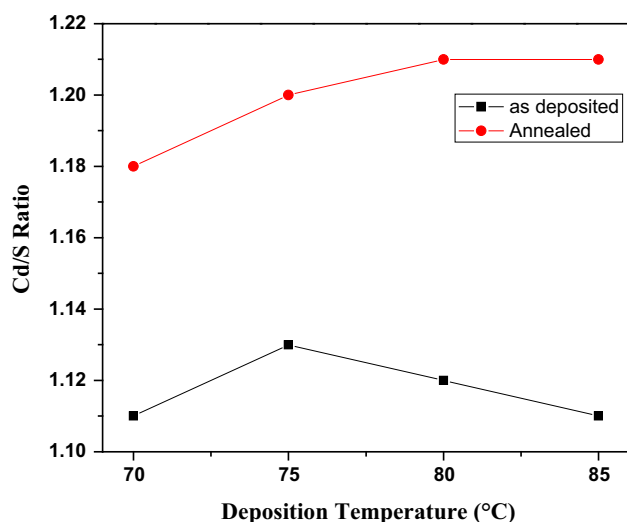


Fig. 1 Atomic ratio of Cd/S for as deposited and annealed CdS thin films

3.2 Structural properties

The XRD patterns of the films (as deposited and annealed) at different deposition temperatures are shown in Fig. 2a, b. Figure 2a belongs to the as deposited CdS films whereas Fig. 2b belongs to the similar samples after annealing in air at 400 °C for 20 min. The spectra were obtained by scanning 2θ in the range 10–60°, with a step resolution equal to 0.02°. The identification and assignments of the observed diffraction patterns were made using the JCPDS data and reported literature [23]. As is well known, CdS can exist in two crystalline modifications: the hexagonal (wurtzite) phase and the cubic (zincblende) phase. For solar cell application, hexagonal CdS films are preferable due to its excellent stability [24]. The results of X-ray analysis agreed well with the earlier reported results [8, 23]. In Fig. 2a, the diffraction patterns showed three diffraction peaks at 26.7°, 44.3°, and 52.3° which correspond to the (111), (220), and (311) planes of the cubic CdS structure. In addition, peaks with peak intensities are seen at 24.77°, 28.18° and 48.02° which are ascribed to the hexagonal phase of CdS. This indicates the coexistence of both the cubic phase and the hexagonal phase in the as deposited films. The integrated areas under the most intense peaks of both the phases were calculated and it was seen that the percentage of the hexagonal phase varies from 13 to 18 % for the as prepared films. The intensity of the hexagonal phase was seen to increase after annealing the films at 400 °C. Areas were calculated similarly and it was seen that the percentage of the hexagonal phase varied from 27 to 33 %. It is well known that the hexagonal phase is thermodynamically more stable, and invariably forms if the cubic phase is heated above 300–400 °C. The low-temperature chemical deposition method therefore can allow the formation of the cubic phase, and this phase is commonly obtained in chemically deposited CdS films. Very often, a mixture of wurtzite and zincblende phases has been reported in the literature.

It is worth noting that the broadening of the XRD diffraction peaks can be due to the crystallite grain size and (or) to the stress in the grain. The crystallite size (D) of the grains can be estimated from the full-width half-maximum (FWHM) values of the diffraction peaks. An average crystallite size (D) in the films has been evaluated by using Scherrer's formula [25].

$$D = \frac{K\lambda}{\beta \cos(\theta)}, \quad (1)$$

where K is a constant (0.94), λ the wavelength of the X-ray, β broadening of diffraction line measured at the half of its maximum intensity (in radian), and θ Bragg's diffraction angle. The variation of the measured grain size of as deposited and annealed CdS thin films with the deposition temperature is reported in Fig. 3. It can be seen from

Fig. 2 X-ray diffraction spectrum of the CdS films under different deposition temperatures **a** as deposited films, **b** annealed at 400 °C

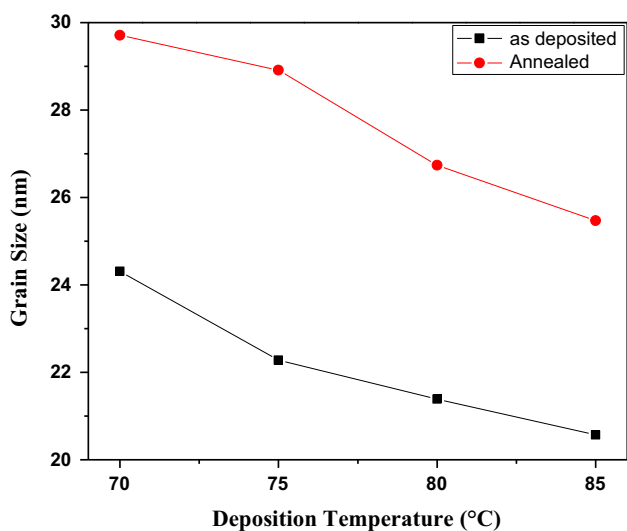
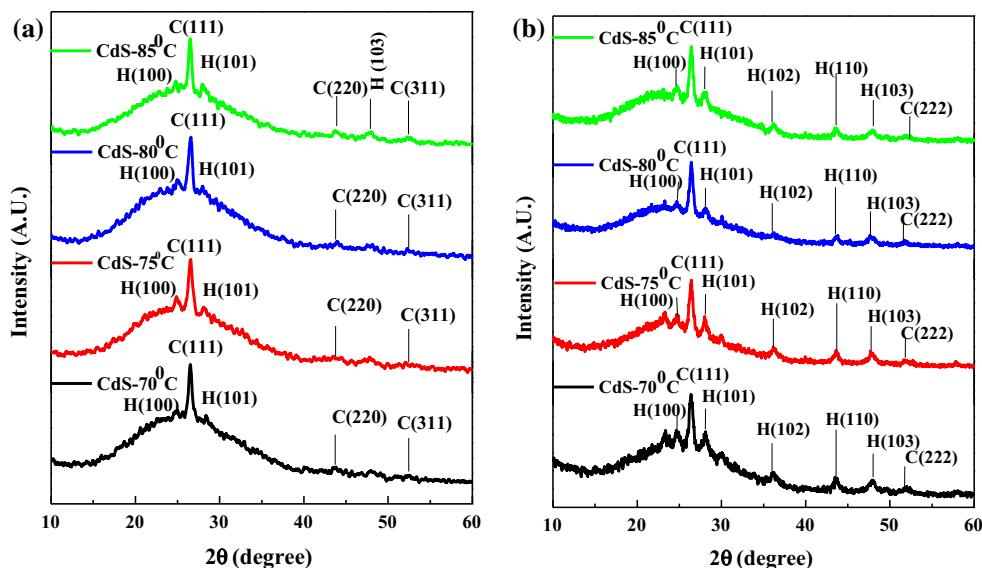


Fig. 3 Variation of grain size as a function of deposition temperature

Fig. 3, the grain size decreases with the increasing deposition temperature. Such behavior has also been observed by Wenyi et al. [13] in CdS thin films deposited at different temperatures. Reduction in the grain size with the increasing deposition temperature indicates that the smoother surface morphology could be obtained with elevated temperature as pointed out before [13].

The dislocation density (δ), which gives direct information about the defects in the crystal structure, can be calculated using the relation [29, 30]

$$\delta = \frac{1}{D^2}, \tag{2}$$

The dislocation density is defined as the “length of dislocation lines per unit volume of the crystal,” and higher

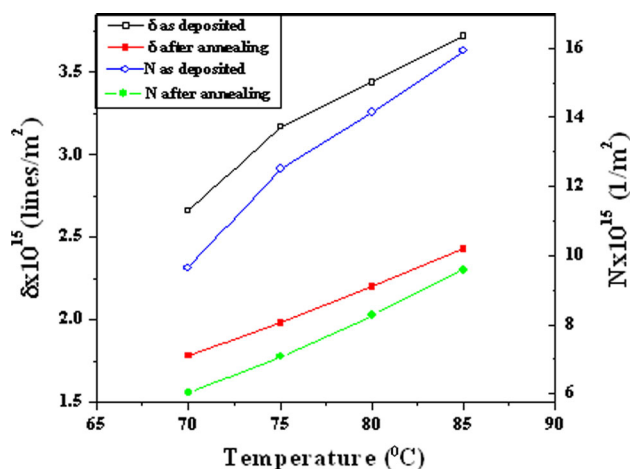


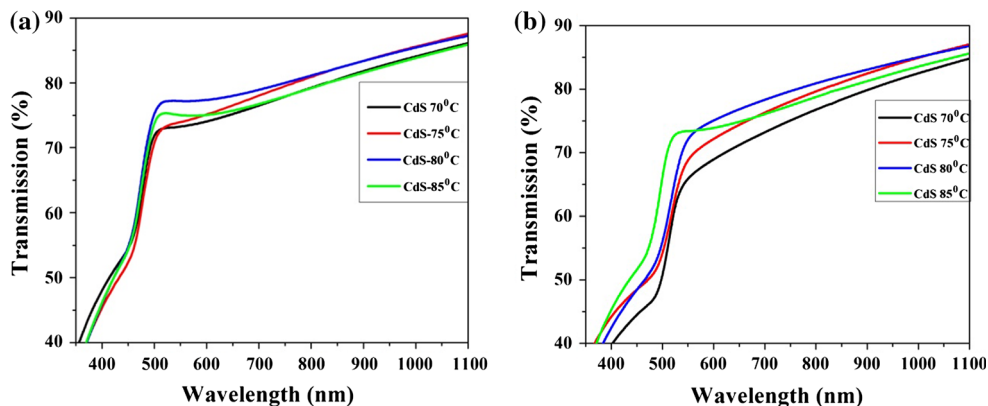
Fig. 4 Variation of dislocation density and number of crystallites per unit area as a function of deposition temperature

values of δ indicate lower crystallinity levels for the films. Furthermore, the number of crystallites per unit area (N) is calculated by using the formula:

$$N = \frac{t}{D^3}, \tag{3}$$

where t is the thickness of the films. The variation of the calculated δ and N of as deposited and annealed CdS thin films with the deposition temperature is shown in Fig. 4. It can be seen that both the parameters δ and N increases with the deposition temperature which gives the indication that by increasing the deposition temperature the defects are increasing. However; significant reduction in both the parameters (δ and N) can be observed by heat treatment or annealing of the as deposited films. Hence, one can conclude that annealing improved the properties of the CdS

Fig. 5 UV–visible transmittance spectra of the CdS films **a** as deposited films, **b** annealed at 400 °C with various deposition temperatures



thin films, which will be confirmed in subsequent sections by further studies and discussions.

3.3 Optical properties

The optical transmittance spectra of (a) as deposited and (b) annealed CdS thin films, in the wavelength range of 350–1100 nm, are shown in Fig. 5. It can be clearly noticed that all the CdS films (as-deposited and annealed) showed good optical properties with high transmittance (>80 %). The transmittance of the films was found to be slightly decreasing after annealing; which may be because of increased roughness of the films which causes scattering of light [26]. In conclusion, all the films have high transmission in the visible region, so that these films could be used as the buffer material in solar cells.

Furthermore, the absorption coefficient α of the thin films was calculated from the transmittance spectra using Beer-Lambert's law. The variation of the coefficient of absorption with the wavelength energy was used to calculate the film optical gap E_g . A plot of $(\alpha h\nu)^2$ and photon energy ($h\nu$) is shown in Fig. 6a, b for the as deposited and annealed CdS thin films. The linear dependence of $(\alpha h\nu)^2$ with $h\nu$ was indicative of the direct band gap material. The

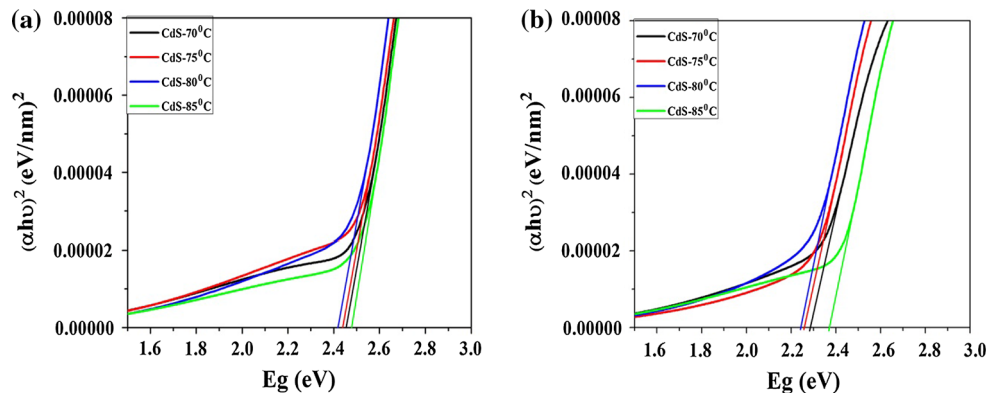
band gap energy E_g was determined by extrapolating the straight line to the energy axis whose intercept to the x-axis gives the optical band gap.

The calculated band gap energy of the as deposited CdS films was found in the range of 2.41–2.47 eV, which is in good agreement with the reported literature [8, 21, 23]. On the other hand, decrease in the band gap values have been observed in the annealed thin films as compare to the as-deposited CdS films. The probable reason may be during annealing temperature decomposition of hydroxides, which reduce the bandgap, similar observation have been recently reported by Ahmad et al. [23].

3.4 Surface morphology

Morphology of the as deposited and annealed films were studied by AFM and FE-SEM. However the TEM analysis was used to confirm the particle size of the deposited nanocrystals. The AFM images are shown in Fig. 7(i) as deposited CdS films (a–d) and (ii) annealed CdS films (e–h). It can be seen that with increase in deposition temperature the CdS films showed the smoother and compact structure [see Fig. 7(i) (a–d)]. This can be because of increased nucleation and deposition rates, with increasing deposition temperatures [8]. Figure 7(ii) (e–h) shows the globular morphology

Fig. 6 Optical band gap for **a** as deposited CdS films **b** annealed CdS films



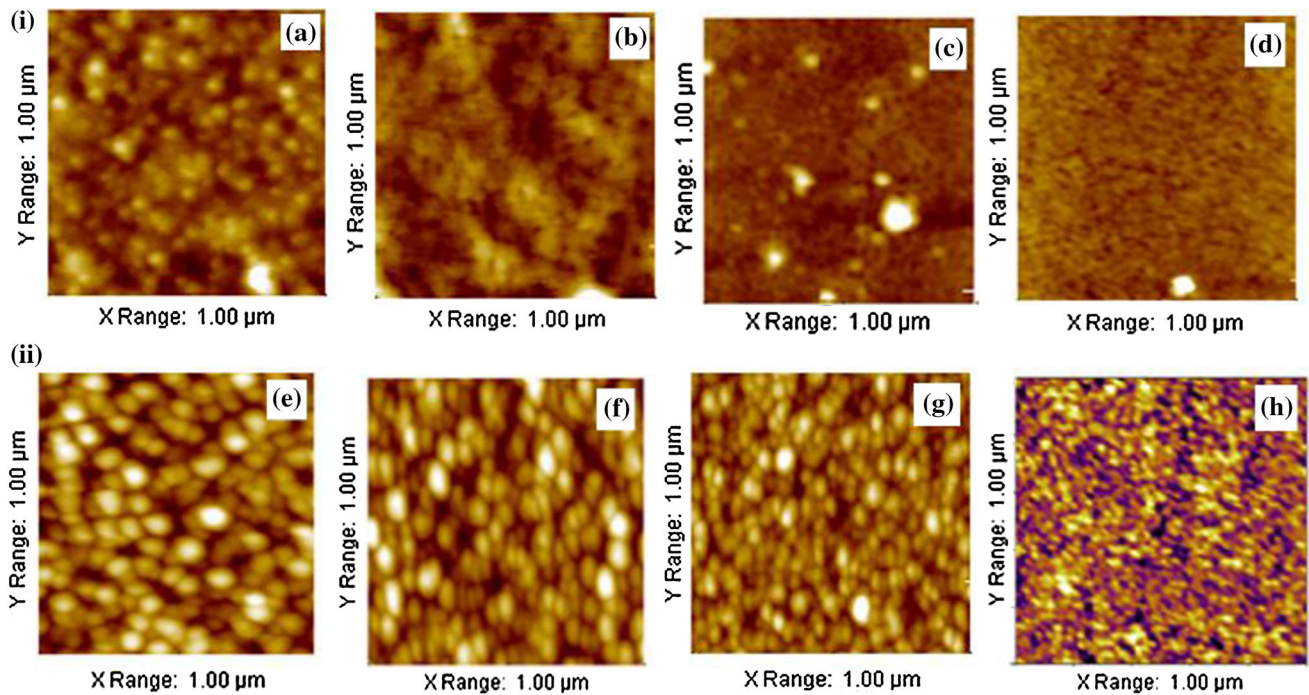


Fig. 7 AFM images of CdS films deposited at 70, 75, 80 and 85 °C. (i) As deposited CdS films (a–d) and (ii) annealed CdS films (e–h)

Table 1 Roughness of CdS films deposited at different temperatures before and after annealing

Sample name (°C)	Roughness (nm) as deposited CdS films	Roughness (nm) after annealing CdS films
CdS-70	8.9	27.4
CdS-75	6.8	18.5
CdS-80	5.1	13.8
CdS-85	4.6	11.2

of the CdS films after annealing. The particles form aggregates because of coalescence of small grains to form spherical clusters. Thus annealing causes strain relaxation and creation of pinholes [7]. After annealing particles adopted sharper edges and increased grain size than as deposited films [21]. The roughness values of the CdS films on 25 μm² area are given in Table 1. Slight decrease in the roughness values were observed with increasing the deposition temperature, which is consistent with the reported literature [13]. However; the roughness values increased remarkably after annealing because annealing acts as thermal etching of the film surface [27]. During annealing agglomerated particles are formed due to coalescence of small grain together, this also led to increased roughness value [21].

The TEM images of annealed CdS films (deposited at 70 °C) are shown in Fig. 8a, b. The particle sizes obtained from the micrograph is about 30 nm which is in good agreement with the sizes calculated from Scherrer equation. A close-up of the particle shows a deviation from

spherical shape which might be a result of fast nucleation and growth of the CdS nanoparticles on the surface of the surface.

The SEM images of as deposited and annealed CdS films at different deposition temperatures are shown in Figs. 9, 10. It can be seen that as grown films are uniform and having spherical morphology of CdS particles. The coverage area increases with increase in deposition temperature. Annealing the films in air atmosphere causes some small pores to appear which may be due to release of hydroxide molecules from the film at high annealing temperature, subsequently results structural change as well as changes in the crystalline property of the film. Annealing of CdS thin films above 300 °C and subsequent pores formation have been reported previously [23, 27]. It has also confirmed with the XRD that phase transformation (cubic to hexagonal phase) in CdS thin film takes place after higher temperatures annealing, this may also contribute in formation of pores [28].

3.5 Electrical properties

The electrical resistivity of as deposited and annealed CdS thin films have been measured using four point probe method. The obtained results are shown in Fig. 11. It can be noticed that electrical resistivity of the films decreases with increase in the deposition temperature however the significant decrease in resistivity can be observed after

Fig. 8 HR-TEM images of after annealed as deposited **a** 70 °C CdS films **b** Enlarge view of the film

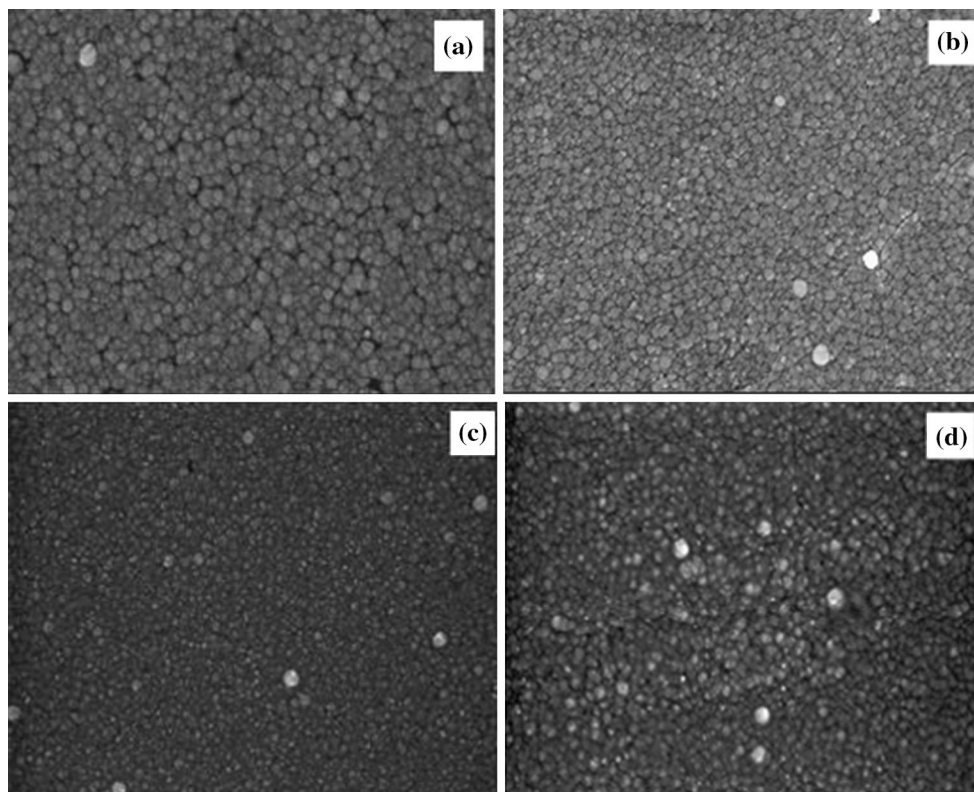
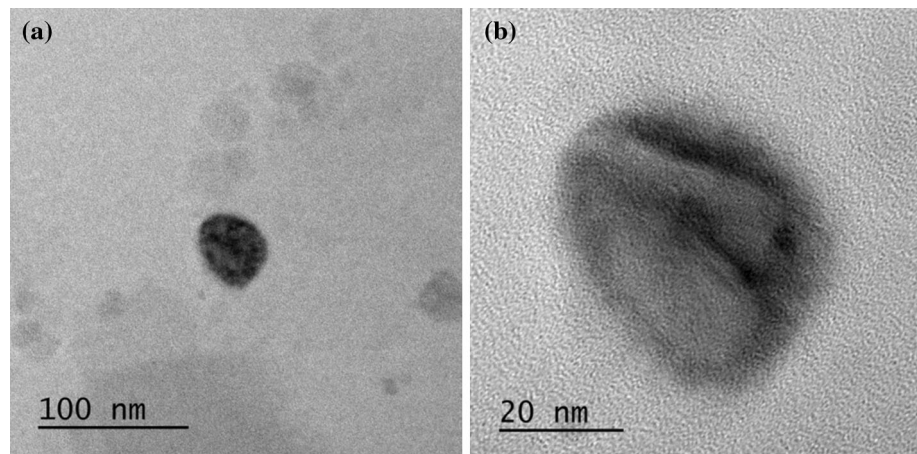


Fig. 9 FE-SEM images of as deposited CdS films at **a** 70 °C, **b** 75 °C, **c** 80 °C and **d** 85 °C

annealing the as deposited CdS thin films. Resistivity of as deposited films found to be in the range of 3.3×10^5 to $9.4 \times 10^4 \Omega\text{-cm}$, our measured values of resistivity are well in agreement with the reported literature [14]. The resistivity further decreases approximately to 10 times after annealing the as-deposited CdS thin films, which indicates the remarkable enhancement of electrical conductivity after annealing. The increased conductivity after annealing can

be related to increased Cd/S ratio. As it is known that annealing of CdS films increases the density of sulfur vacancies, subsequently the Cd/S ratio of the films increased. Increase in the carrier concentration due to the increase in the density of sulfur vacancies after annealing above 300 °C has been recently reported by Ahmad et al. [23]. In conclusion, electrical conductivity of the CdS films can be enhanced by heat treatment at appropriate temperature.

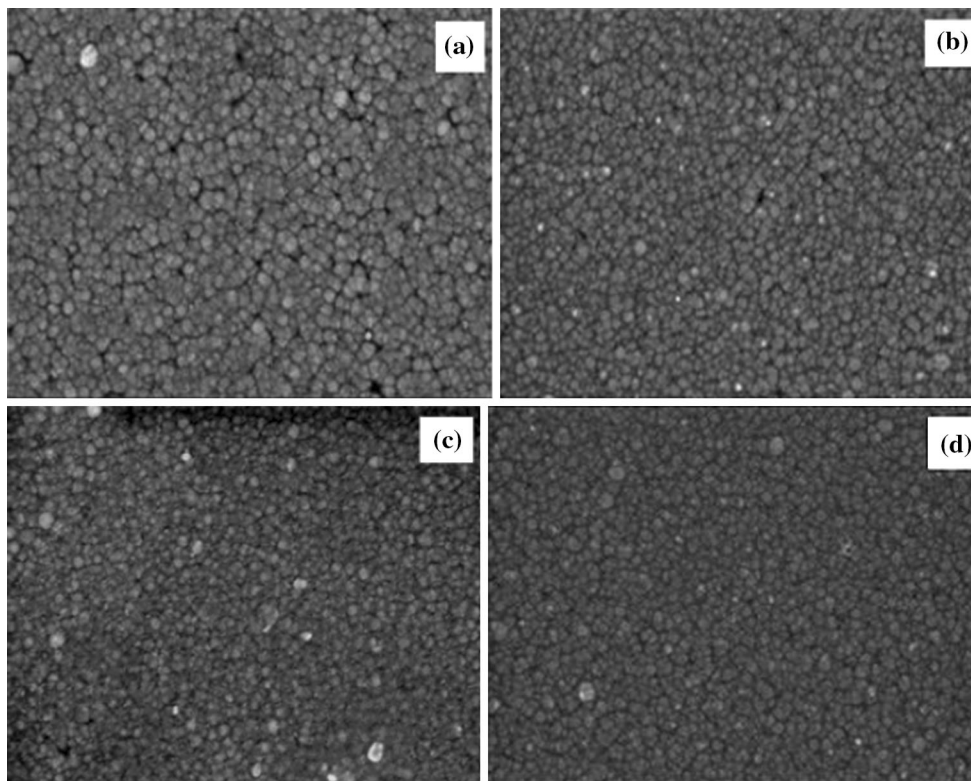


Fig. 10 FE-SEM images of after annealing as deposited CdS films **a** 70 °C, **b** 75 °C, **c** 80 °C and **d** 85 °C

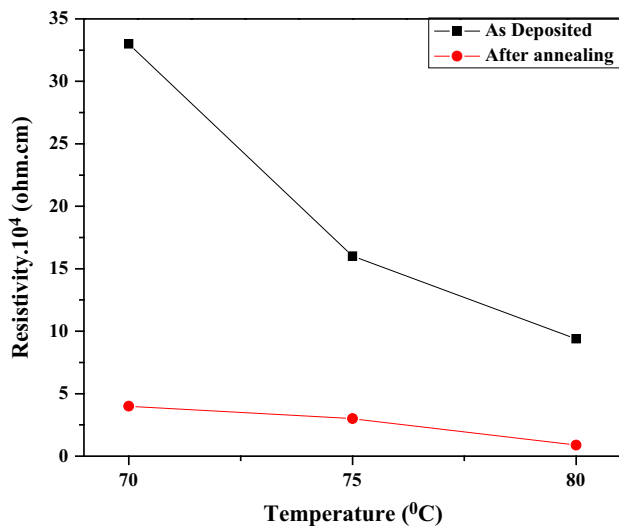


Fig. 11 Electrical resistivity of as deposited and annealed CdS films as a function of deposition temperature

4 Conclusion

The structural, morphological, electrical and optical properties of chemically bath deposited films were investigated. The effect of annealing and deposition temperature on these films characteristics have been thoroughly studied

and found that annealing may improve all the properties of the as deposited films. XRD patterns of these films clearly show the transformation of CdS film from the cubic structure to the stable hexagonal structure. All the films grown at different deposition temperatures had very good transmittance. The band gaps after annealing found to decrease due to decay of hydroxides. The electrical conductivity after annealing the as-deposited thin films found to increase; the sulfur vacancies are mainly responsible for contributing carriers for conduction.

Acknowledgment The authors Dipti Desai and Ravi Kant Choubey are thankful to Department of Science & Technology, Science & Engineering Research Board, New Delhi for the financial support (Grant No. SR/FTP/PS-038/2012). One of the authors Ravi Kant Choubey is also thankful to Defence Institute of Advanced Technology, Girinagar, Pune for the financial support (Grant No. DAIT/F/REG(G)/BS/Proj/2014/2).

References

1. Y.D. Chung, D.H. Cho, N.M. Park, K.S. Lee, J. Kim, *Curr. App. Phys.* **11**, S65 (2011)
2. J. Ayre, New CIGS Solar Cell Record: 21.7% CIGS Cell Conversion Efficiency Achieved at ZSW, <http://cleantechnica.com>. Accessed 27 Sept 2014
3. B. Moon, J. Lee, H. Jung, *Thin Solid Films* **511–512**, 299 (2006)

4. A. Hartley, S.J.C. Irvine, D.P. Halliday, M.D.G. Potter, *Thin Solid Films* **387**, 89 (2001)
5. M. Hadrich, N. Lorenza, H. Metznera, U. Reislohnera, S. Macka, M. Gossila, W. Witthuhn, *Thin Solid Films* **515**, 5804 (2007)
6. N. Romeoa, A. Bosio, V. Canevarib, M. Terheggenc, L.V. Roca, *Thin Solid Films* **431–432**, 364 (2003)
7. A. Romeoa, D.L. Batznera, H. Zogga, C. Vignalib, A.N. Tiwari, *Sol. Energy Mater. Sol. Cells* **67**, 311 (2001)
8. Y.S. Lo, R.K. Choubey, W.C. Yu, W.T. Hsu, C.W. Lan, *Thin Solid Films* **520**, 217 (2011)
9. R.K. Choubey, S. Kumar, C.W. Lan, *Adv. Nat. Sci. Nanosci. Nanotech.* **5**, 025015 (2014)
10. K. Ravichandran, P. Philominathan, *Sol. Energy* **82**, 1062 (2008)
11. K.P. Acharya, K. Mahalingam, B. Ullrich, *Thin Solid Films* **518**, 1784 (2010)
12. N. Romeo, A. Bosio, V. Canevari, A. Podesta, *Sol. Energy* **77**, 795 (2004)
13. Li Wenyi, Cai Xun, Chen Qiulong, Zhou Zhibin, *Mater. Lett.* **59**, 1 (2005)
14. A. Kariper, E. Guneri, F. Gode, C. Gumus, T. Ozpozan, *Mat. Chem. Phys.* **129**, 183 (2011)
15. H. Metin, R. Esen, *Semicond. Sci. Technol.* **18**, 647 (2003)
16. O. Vigil, O. Zelaya-Angel, Y. Rodriguez, *Semicond. Sci. Technol.* **15**, 259 (2000)
17. J. Han, L. Cheng, T. Jiang, G. Fu, V. Krishnakumar, C. Spanheimer, G. Haindl, K. Zhao, A. Klein, W. Jaegermann, *Mater. Res. Bull.* **46**, 194 (2011)
18. B. Liu, R. Luo, Q. Lian, Y. Zheng, B. Li, J. Zhang, W. Li, L. Wu, L. Feng, *J. Mater. Sci. Mater. Electron.* **26**, 9985 (2015)
19. J.K. Cooper, J. Cao, Jin Z. Zhang, *ACS Appl. Mater. Interfaces* **5**, 7544 (2013)
20. R. Premarani, J.J. Devadasan, S. Saravanakumar, R. Chandramohan, T. Mahalingam, *J. Mater. Sci. Mater. Electron.* **26**, 2059 (2015)
21. A. Cortes, H. Gomez, R.E. Marotti, G. Riveros, E.A. Dalchiale, *Sol. Energy Mater. Sol. Cells* **82**, 21 (2004)
22. C. Guillen, M.A. Martinez, C. Maffiotte, J. Herrero, *J. Electrochem. Soc.* **148**, G602 (2001)
23. F.R. Ahmad, A. Yakimov, R.J. Davis, J.H. Her, J.R. Courmoyer, N.M. Ayensu, *Thin Solid Films* **535**, 166 (2013)
24. C.Y. Yeh, Z.W. Lu, S. Froyen, A. Zunger, *Phys. Rev. B* **46**, 10086 (1992)
25. B.D. Cullity, *Elements of X-ray Diffraction*, 2nd edn. (Addison-Wesley, Reading, MA, 1978)
26. S.H. Mohamed, M.E. Hagary, M.E. Ismail, *J. Phys. D Appl. Phys.* **43**, 075401 (2010)
27. J. Hiie, K. Muska, V. Valdna, V. Mikli, A. Taklaja, A. Gavrilov, *Thin Solid Films* **516**, 7008 (2008)
28. H. Ariza-Calderon, R. Lozada-Morales, O. Zelaya-Angel, J.G. Mendoza-Alvarez, L. Banos, *J. Vac. Sci. Technol. A* **14**, 2480 (1996)
29. M. Robert Jr., D.L. Morel, C.S. Ferekides, *Thin Solid Films* **484**, 26 (2005)
30. W.D. Callister, *Materials Science and Engineering—An Introduction* (Wiley, New York, 1997)